Arthritis Research & Therapy

RESEARCH

Open Access

Regional brain function study in patients with primary Sjögren's syndrome

Chunfeng Hu[1†], Luoyu Wang[1,2†], Jiao Huang[3], Yushan Shang[4], Xiaofang Zhang[3], Xinyun Du[3], Huijun Cao[5], Zhijiang Han[1*] and Peiying Wei[1*]

Abstract

Background Primary Sjögren's syndrome (pSS) manifests a spectrum of neuropsychological symptoms, primarily cognitive impairment, but the mechanism of central nervous system damage remains unclear. This study sought to analyze differences in the static and dynamic fractional amplitude of low-frequency fluctuation (fALFF) and region homogeneity (ReHo) between pSS patients and healthy controls (HCs), aiming to elucidate regional brain function alterations and investigate underlying mechanisms.

Methods Using stringent inclusion and exclusion criteria, 68 pSS patients and 69 HCs were assessed, including rs-fMRI, neuropsychological assessments, and laboratory tests. Static fALFF (sfALFF), static ReHo (sReHo), dynamic fALFF (dfALFF), and dynamic ReHo (dReHo) were calculated separately using two-sample *t*-tests to identify differences in brain regions between the two groups. Correlations between these regions and disease duration, laboratory indicators, and neuropsychological test scores were also examined.

Results Static index analysis revealed increased sfALFF in the right supplementary motor area in pSS patients, with significant decreases in sReHo in the left orbital media frontal gyrus, left caudate nucleus, and right precuneus lobe. Dynamic index analysis showed significant increases in dfALFF in the left supplementary motor area and dReHo in the right dorsolateral superior frontal gyrus. Furthermore, sReHo in the right precuneus lobe negatively correlated with NCT-A scores ($P=0.005$), and dReHo in the right dorsolateral superior frontal gyrus negatively correlated with DST scores ($P=0.007$).

Conclusion PSS patients experience notable changes in regional brain function, as evidenced by alterations in both static and dynamic brain indicators. Integrating these metrics provides a holistic view of the brain function alterations in pSS patients.

Keywords Primary Sjögren's syndrome, Resting-state functional magnetic resonance imaging, Cognitive impairment, Regional brain function

[†]Chunfeng Hu and Luoyu Wang contributed equally to this work.

*Correspondence:
Zhijiang Han
hanzhijiang@hospital.westlake.edu.cn
Peiying Wei
b2018184@zju.edu.cn
[1]Department of Radiology, Affiliated Hangzhou First People's Hospital, Westlake University School of Medicine, Hangzhou, China
[2]School of Biomedical Engineering, Shanghai Tech University, Shanghai, China
[3]Department of Rheumatology, Affiliated Hangzhou First People's Hospital, Westlake University School of Medicine, Hangzhou, China
[4]Department of Clinical Psychology, Affiliated Hangzhou First People's Hospital, Westlake University School of Medicine, Hangzhou, China
[5]The Fourth Clinical College, Zhejiang Chinese Medical University, Hangzhou, China

Background

Primary Sjögren's syndrome (pSS), an autoimmune pathology marked by lymphocytic proliferation and exocrine gland deterioration, often extends beyond glandular dysfunction to systemic and multi-organ afflictions [1], with the central nervous system (CNS) being a significant non-glandular target exhibiting incidence rates from 10 to 60% [2–5]. The clinical spectrum of pSS ranges from minor cognitive disturbances to severe cerebrovascular events [5–9], critically affecting patient morbidity and mortality. Despite its prevalence, the mechanisms driving CNS compromise in pSS remain poorly understood, exacerbated by the absence of standardized diagnostic criteria [7, 8], particularly during initial stages when symptoms like cognitive decline may be subtle. We will attempt an applicable diagnostic method to explore the mechanism related to early detection and prognosis of CNS involvement in individuals with pSS.

Resting-state Functional Magnetic Resonance Imaging (rs-fMRI) is currently the most widely used non-invasive functional imaging technique, offering advantages such as ease of operation, high patient acceptance, and excellent stability and repeatability [10, 11]. It detects spontaneous neural activity by measuring low-frequency fluctuations in blood oxygen level-dependent (BOLD) signals, providing insights into brain function [12]. The analysis of rs-fMRI typically encompasses two primary methodologies: functional integration and functional segregation. Functional integration examines the interactions among diverse time series signals and is widely applied in the study of neurological disorders [13–15]. However, while it reveals comprehensive connectivity abnormalities, it lacks the granularity to pinpoint specific affected brain regions. To address this, Zang et al. introduced the Amplitude of Low-Frequency Fluctuations (ALFF) and Regional Homogeneity (ReHo) metrics [16, 17], which focus on regional spontaneous neuronal activity (i.e., functional segregation). This approach analyzes individual voxel or local region signals, facilitating the identification of precise brain areas affected by neurological conditions. Compared to integration analysis, functional segregation analysis offers simpler operations and yields results with enhanced interpretability and specificity.

The ALFF value reflects the magnitude of fluctuation amplitude of each voxel's individual time series signal, indicating the intensity of local spontaneous brain activity. Currently, only Zhang et al. [8] have employed ALFF analysis to study Sjögren's syndrome. However, this method has limitations, as it can be influenced by non-neurophysiological fluctuations such as respiration, cardiac activity, cerebrospinal fluid movement, and vascular pulsation [18]. To address these limitations, the Fractional Amplitude of Low-Frequency Fluctuation (fALFF) was developed. fALFF assesses the relative contribution of specific ALFF to the entire frequency range [19] and effectively reduces the influence of physiological noise, thereby improving the specificity and sensitivity of detecting spontaneous neural activity signals [20]. However, to date, no scholars have employed the fALFF analysis method to study regional brain functional changes in pSS patients. ReHo is another measure used to assess the consistency of regional brain functional activity [21]. Although Xing et al. [22] have employed ReHo to explore central functional changes in pSS patients, their study suffered from a small sample size and limited generalizability. Moreover, existing research has relied on the assumption of signal stationarity during scanning, neglecting the dynamic temporal changes in spontaneous brain activity, which may result in the oversight of critical information. In light of these limitations, our study adopts a combined static and dynamic approach, utilizing both fALFF and ReHo analyses and expanding the sample size to robustly investigate CNS functional changes in pSS patients. This methodology aims to provide a more comprehensive understanding of the neural underpinnings of pSS, incorporating both static and time-varying aspects to capture a fuller spectrum of neural dynamics.

Specifically, this study combines static fALFF (sfALFF) and static ReHo (sReHo) with dynamic fALFF (dfALFF) and dynamic ReHo (dReHo) to analyze regional brain functional changes in pSS patients, aiming to elucidate the central mechanisms involved. Our hypotheses are as follows: (1) there are observable modifications in sfALFF and sReHo across multiple cerebral regions in pSS subjects; (2) variations in dfALFF and dReHo also manifest across several brain regions, offering additional insights when compared with static indices; (3) specific cerebral regions demonstrating these changes may be linked to the psychosocial manifestations associated with pSS. This comprehensive analysis seeks to enhance the understanding of the brain's role in the pathophysiology of pSS and potentially guide therapeutic strategies.

Methods

Participants

This study prospectively collected clinical and imaging data of pSS patients at the Rheumatology and Immunology Department of the First People's Hospital of Hangzhou from March 2021 to August 2023. Approval was obtained from the Research Ethics Committee (2021-023-01 and ZN-20230331-0053-01), adhering to the Helsinki Declaration, with all participants providing written informed consent.

Inclusion criteria for pSS patients were as follows: (1) Patients diagnosed with pSS according to the European-American consensus criteria; (2) Absence of psychiatric and psychological disorders prior to pSS diagnosis;

(3) Absence of other connective tissue diseases such as systemic lupus erythematosus, antiphospholipid syndrome, systemic sclerosis, and rheumatoid arthritis; (4) Age between 20 and 75 years; (5) Right-handedness; (6) Absence of motor, auditory, and visual system disorders, no language barriers, and normal corrected vision; (7) Voluntary participation in the study.

Inclusion criteria for healthy controls (HCs) were: (1) Age between 20 and 75 years; (2) Right-handedness; (3) Good physical condition, no history of tumors or psychiatric disorders; (4) Absence of motor, auditory, and visual system disorders, no language barriers, and normal corrected vision; (5) Voluntary participation in the study.

Exclusion criteria were: (1) Severe hypertension, diabetes, and other diseases affecting brain function; (2) Previous history of cerebral organic lesions, head trauma, or invasive surgery; (3) Contraindications to MRI scans; (4) History of alcohol dependence or substance abuse.

After quality control assessment, 68 pSS patients and 69 HCs were included in the final analysis following the exclusion of invalid data (Fig. 1).

Disease duration, disease activity assessment, and neuropsychological assessments

The time of the first diagnosis of pSS was defined as the onset of the disease. Therefore, the disease duration was calculated as the period from disease onset to inclusion in the study.

The extent of inflammatory activity in systemic tissues and organs caused by pSS is referred to as disease activity. In this study, disease activity was assessed using the EULAR Sjögren's Syndrome Disease Activity Index (ESSDAI), developed by the European League Against Rheumatism in 2009. The ESSDAI evaluates disease activity across twelve domains: systemic symptoms, lymph nodes, joints, glands, skin, lungs, kidneys, muscles, central nervous system, peripheral nervous system, hematological system, and serological markers. The total score reflects the overall disease activity of the patient. Higher scores in a specific domain or overall indicate greater disease activity in that domain or the entire system.

All participants underwent a series of neuropsychological tests within 2 h after the MRI examination. Cognitive function was evaluated using the Mini-Mental State Examination (MMSE). Anxiety and depression states were assessed using the Self-Rating Anxiety Scale (SAS) and the Self-rating Depression Scale (SDS), respectively. Attention and information processing speed assessed using with the Digit Symbol Test (DST), whereas psychomotor ability was evaluated with the Number Connection Test-Type A (NCT-A). All assessments were conducted by the same physician to ensure consistency.

MRI parameters

Participants underwent MRI data acquisition using a 3.0 T MRI scanner (Siemens, MAGNETOM Verio, Germany) with an 8-channel phased-array head coil. They were instructed to remain awake with their eyes closed and to wear foam pads and earplugs to minimize head motion and scanner noise interference.

Initial scans included T1-weighted imaging (T1WI), T2-weighted imaging (T2WI), T2 fluid attenuated inversion recovery (T2 FLAIR), and diffusion-weighted imaging (DWI) to rule out intracranial pathologies, with the following parameters: T1WI: repetition time (TR)/

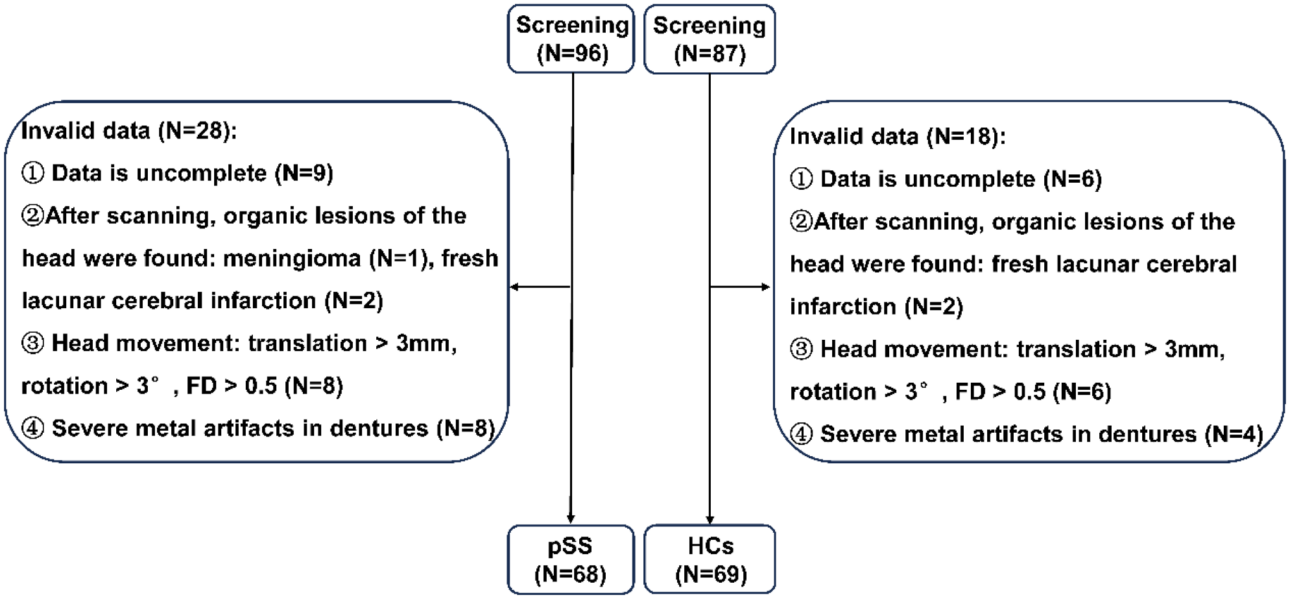

Fig. 1 Exclusion of invalid data. FD, Framewise displacement

echo time (TE) = 500ms/8.5ms, matrix = 120 × 256, field of view (FOV) = 230 mm×230 mm, slice thickness = 5 mm, slice gap = 1.5 mm, number of slices = 20. T2WI: TR/TE = 5000ms/117ms, matrix = 248 × 320, FOV = 220 mm×220 mm, slice thickness = 5 mm, slice gap = 1 mm, number of slices = 20. T2 FLAIR: TR/TE = 8000ms/94ms, matrix = 186 × 256, FOV = 230 mm×230 mm, slice thickness = 5 mm, slice gap = 1 mm, number of slices = 20. DWI: TR/TE = 5100ms/100ms, matrix = 192 × 192, FOV = 230 mm×230 mm, slice thickness = 5 mm, slice gap = 0.4 mm, number of slices = 20, b-value = 1000s/mm².

Anatomy images were obtained using a three-dimensional T1-weighted imaging (3D-T1WI) sequence with the following parameters: TR = 1900ms, TE = 2.52ms, inversion time = 900ms, flip angle = 9°, FOV = 256 mm×256 mm, slice thickness/slice gap = 1/0 mm, matrix = 256 × 256, with a total of 176 sagittal slices.

Rs-fMRI data were acquired using a gradient-echo imaging sequence with the following parameters: TR = 2000ms, TE = 30ms, slice thickness/slice gap = 3.2/0 mm, FOV = 220 mm×220 mm, flip angle = 90°, with 250 time points collected per scan.

Image preprocessing

Examine the quality of all 3D-T1WI and rs-fMRI images, excluding incomplete or artifact-affected images. Rs-fMRI data preprocessing utilized the Data Processing and Analysis of Brain Imaging (DPABI) 6.2 toolbox on MATLAB (2018b, MathWorks, Natick, MA, United States).

The following were the specific image preprocessing steps: (1) Removal of the first 10 time points of each rs-fMRI dataset to ensure MRI signals reached a stable state; (2) Temporal alignment of the remaining rs-fMRI data; (3) Correction of head motion, while excluding subjects with maximum head displacement exceeding 3 mm, rotation exceeding 3°, or frame-wise displacement exceeding 0.5; (4) Registration of the subject's structural image to the corresponding mean functional image; (5) Segmentation of the registered structural image into gray matter, white matter, and cerebrospinal fluid to obtain registration matrices between the mean functional image and the standard space; (6) Transformation of subject data from the original space to the Montreal Neurological Institute standard space by applying the registration matrices onto the functional image, with voxel size resampled to 3 mm×3 mm×3 mm; (7) Removal of linear drift by linear regression to eliminate signal changes due to machine heating during continuous operation; (8) Regression of covariates, including Friston-24 head motion parameters, cerebrospinal fluid signal, and white matter signal; (9) Band-pass filtering of rs-fMRI data using a 0.01 ~ 0.08 Hz bandpass filter to remove low-frequency linear drift and high-frequency physiological noise such as respiration and heartbeat, with this step specifically applied for ReHo value calculation.

Static indicators calculation

A fast Fourier transform was performed on whole-brain voxels to convert the BOLD signal into the frequency-domain power spectrum. The square root of the power spectrum was calculated at each frequency, and the average value within the range of 0.01 to 0.08 Hz was used to calculate the sfALFF metric. sReHo values were calculated using Kendall's coefficient of concordance method, which assesses the temporal synchronization between the time series of a voxel and its 26 neighboring voxels to generate whole-brain sReHo values for each participant. To ensure comparability, sfALFF and sReHo values of individual voxels were normalized to the mean values of the entire brain. Spatial smoothing was applied using a Gaussian kernel with a full width at half maximum (FWHM) of 6 mm to minimize incomplete registration and improve the image signal-to-noise ratio, thereby improving the reliability of the results.

Dynamic indicators calculation and validation

The analysis of dfALFF and dReHo was performed using the DPABI-based dynamic analysis toolbox. Dynamic indicators were calculated using a sliding window approach, recognized for its sensitivity in detecting temporal changes and assessing whole-brain indicator variability [23]. The length of the sliding window is a critical parameter. It should be sufficiently large to enable robust analysis of the lowest frequencies of interest in the signal, yet small enough to capture transient signals [24]. For our analysis, a sliding window length of 50 TRs (100s) was used, with a moving step of 2 TRs (4s). Subsequently, the standard deviation of fALFF and ReHo for each voxel within the time window was calculated to generate the dfALFF and dReHo matrices, which characterize the dynamic variations in fALFF and ReHo. Lastly, consistent with the static indicators, spatial smoothing was performed using a Gaussian kernel with an FWHM of 6 mm.

To ensure the reliability of the results, dfALFF and dReHo results were further validated using dynamic methods with sliding window lengths of 50 TRs (100s) and moving steps of 5 TRs (10s), as well as sliding window lengths of 100 TRs (200s) with a moving step of 2 TRs (4s).

Statistical analysis

The Shapiro-Wilk test was performed to evaluate the distribution of continuous variables using SPSS 25.0 software. Normally distributed data were presented

as mean ± standard deviation ($\bar{x} \pm s$) and compared between groups using the independent samples t-test. Non-normally distributed data were presented as median (interquartile range) [*M (P25, P75)*] and compared between groups using the Wilcoxon rank sum test. The chi square test is used for inter group comparison of categorical variables. Statistical significance was set at $P < 0.05$. In DPABI software, a two independent samples t-test was used to compare pSS patients and HCs on sfALFF, sReHo, dfALFF, and dReHo indicators within the classic frequency band (0.01~0.08 Hz). Group comparisons were conducted applying Gaussian random-field theory (GRF, voxels $P < 0.001$, clusters $P < 0.05$). sfALFF, sReHo, dfALFF, and dReHo values were extracted from brain regions exhibiting significant differences between pSS and HC groups. Subsequently, partial correlation analysis was used to evaluate the relationships between disease duration, treatment, laboratory indicators, and neuropsychological scores with these significant brain regions. Gender, age, years of education, and head motion were included as covariates in the analysis. Statistical significance was assessed using a Bonferroni-corrected threshold of $P < 0.008$ (0.05/6).

Results

Demographic information, laboratory indicators, and neuropsychological assessments

A total of 68 pSS patients and 69 HCs were included in this study. Categorical variables were compared between the two groups using the chi-square test, and continuous variables were compared using the Wilcoxon rank-sum test. The results showed that the SAS scores in the pSS group were significantly higher than those in the HC group ($P < 0.001$). No statistically significant differences were observed in the remaining parameters (all $P > 0.05$) (Table 1).

Analysis of clinical symptoms (involvement) and treatment status

This study analyzed the clinical symptoms (involvement) of 68 patients with pSS, identifying a total of 20 symptoms. These symptoms included dry mouth ($n = 56$), dry eyes ($n = 40$), dry and itchy skin ($n = 9$), fatigue ($n = 9$), caries ($n = 7$), interstitial lung disease ($n = 7$), hematological abnormalities ($n = 8$), joint pain ($n = 6$), skin erythema ($n = 4$), abnormal renal function ($n = 3$), abnormal liver function ($n = 3$), myalgia ($n = 2$), reduced limb muscle strength ($n = 1$), mouth ulcers ($n = 2$), mumps ($n = 1$), conjunctivitis ($n = 1$), dry and painful external genitalia ($n = 1$), weight loss ($n = 2$), lymphadenopathy ($n = 1$), and threatened abortion ($n = 1$) (Supplementary Figure S1). Some patients presented with multiple symptoms at the onset of the disease.

Among the pSS patients included in this study, 21 patients did not receive treatment prior to MRI, and 47 patients received treatment. Specifically, patients without systemic involvement beyond lacrimal and salivary gland were treated with hydroxychloroquine, total glucosides of paeony, or a combination of both, with

Table 1 Demographic information, laboratory indicators, and neuropsychological tests of all subjects

Characteristics	pSS (*N* = 68)	HCs (*N* = 69)	χ^2/Z value	*P* value
Age (years)	50.22 ± 13.42	54.00 (46.00, 59.00)	-0.612$^{\varphi}$	0.541
Sex (Male/Female)	1/67	1/68	0.000$^{\#}$	0.992
Education (years)	9.00 (6.00, 14.25)	9.00 (6.00, 12.00)	-1.019$^{\varphi}$	0.308
Head motion	0.05 (0.04, 0.09)	0.06 (0.05, 0.09)	-0.263$^{\varphi}$	0.793
Disease duration (months)	12.00 (0.00, 48.00)	/	/	/
Treatments (yes/no)	47/21	/	/	/
ESSDAI (scores)	2.00 (1.00, 5.00)	/	/	/
MMSE (scores)	29.00 (28.00, 30.00)	29.00 (28.00, 30.00)	-0.581$^{\varphi}$	0.561
SAS (scores)	31.38 ± 5.45	26.00 (24.00, 30.00)	-4.736$^{\varphi}$	**< 0.001***
SDS (scores)	27.00 (22.25, 31.00)	27.00 (23.00, 30.00)	-0.060$^{\varphi}$	0.952
NCT-A (seconds)	47.00 (38.25, 64.50)	47.35 ± 11.97	-0.532$^{\varphi}$	0.595
DST (scores)	37.50 (21.25, 55.00)	34.36 ± 11.51	-1.208$^{\varphi}$	0.227
IgG (g/L)	19.60 (15.15, 22.18)	/	/	/
IgA (g/L)	3.11 ± 1.50	/	/	/
IgM (g/L)	1.36 (0.94, 1.82)	/	/	/
C3 (g/L)	0.81 ± 0.03	/	/	/
C4 (g/L)	0.19 ± 0.00	/	/	/
anti-La/SS-B (negative/ positive)	44/24	/	/	/
anti-Ro/SS-A (negative/ positive)	8/60	/	/	/

Note: pSS, primary Sjögren's syndrome; HCs, healthy controls; ESSDAI, EULAR Sjögren's Syndrome Disease Activity Index; MMSE, Mini-Mental State Examination; SAS, Self-Rating Anxiety Scale; SDS, Self-rating Depression Scale; NCT-A, Number Connection Test-Type A; DST, Digit Symbol Test; $^{\#}$ indicates χ^2 test; $^{\varphi}$ indicates Wilcoxon rank sum test; * indicates a significant level of $P < 0.05$

hydroxychloroquine monotherapy being more common ($n = 28$). While patients with systemic involvement beyond lacrimal and salivary gland were treated with immunosuppressants (e.g., cyclophosphamide, azathioprine and cyclosporine) and appropriate hormone therapy ($n = 19$).

Group differences in SfALFF and sReHo

Compared with the HCs, the pSS group showed significantly higher sfALFF values in the right supplementary motor area (SMA_R) and increased sReHo values in the left orbital middle frontal gyrus (Frontal_Med_Orb_L), left caudate nucleus (CAU_L), and right precuneus lobe (PCUN_R) (GRF; voxel-level $P < 0.001$, cluster-level $P < 0.05$) (Table 2; Fig. 2).

Group differences in DfALFF and dReHo

Compared with the HCs, the dfALFF value of the left supplementary motor area (SMA_L) and the dReHo value of the right dorsolateral superior frontal gyrus (Frontal_Sup_R) in the pSS group showed significant increases (GRF; voxel-level $P < 0.001$, cluster-level $P < 0.05$) (Table 3; Fig. 3). The results remained robust after verification with different sliding window lengths and moving steps (Supplementary Table S1 and Supplementary Figure S2).

Correlations between static and dynamic indicators with disease duration, treatment, laboratory indicators, and neuropsychological assessments

In this study, partial correlation analysis was further employed to investigate the relationships between sfALFF, sReHo, dfALFF, and dReHo values in the aforementioned brain regions and disease duration, treatment, laboratory indicators, and neuropsychological test scores in pSS patients. The results revealed a negative correlation between the sReHo value in the right precuneus and the NCT-A score ($P = 0.005$), as well as a negative correlation between the dReHo value in the right dorsolateral superior frontal gyrus and the DST score ($P = 0.007$). No other significant correlations were found (all $P > 0.008$) (Table 4; Fig. 4). Prior to correction, the sReHo value of PCUN_R demonstrated a negative correlation with C4 ($P = 0.045$), and the dfALFF value of SMA_L demonstrated a positive correlation with anti-SSB antibodies ($P = 0.022$). However, these correlations were no longer significant after correction.

Discussion

This study, for the first time, combines two regional brain functional indices of rs-fMRI (fALFF and ReHo) and integrates static and dynamic indices to explore the central damage mechanism in pSS patients. The findings demonstrate that both static (sfALFF, sReHo) and dynamic (dfALFF, dReHo) neuroimaging metrics reveal significant alterations in multiple brain regions of pSS patients, with no overlap between regions identified by above neuroimaging metrics, indicating that dynamic measures provide complementary insights to static assessments. Furthermore, some metrics in specific brain regions exhibit a negative correlation with neurocognitive scores, underscoring their potential relevance in assessing cognitive impairment. Overall, our study highlights the utility of combining static and dynamic rs-fMRI metrics, offering a more nuanced understanding of functional brain alterations in pSS patients.

Abnormal brain regions in SfALFF and sReHo

fALFF reflects the relative intensity of brain functional activity, with higher values potentially signaling increased activity within a specific frequency range, which may be associated with the importance of that brain region in particular cognitive tasks. ReHo assesses the consistency of regional neural activity within specific brain regions, with higher values indicating greater consistency of activity within that area [20].

The findings of this study reveal an elevated sfALFF value in the SMA_R of pSS patients, indicating a compensatory increase in brain functional activity in this region. Meanwhile, decreased sReHo values in the Frontal_Med_Orb_L, CAU_L, and PCUN_R in pSS patients suggest abnormalities in the internal activity coherence of multiple brain regions.

The supplementary motor area (SMA), first described by Penfield et al. [25], is located in Brodmann area 6 and is part of the sensorimotor network. It is involved in motor planning, execution, language processing, and mental disorder regulation [26–28]. The pre-SMA, a

Table 2 Brain regions with changed SfALFF and sReHo between the pSS and HC groups

Indices	Brain region	MNI coordinate			Voxels	Peak intensity
		X	Y	Z		
sfALFF	SMA_R	9	3	78	54	4.7558
sReHo	Frontal_Med_Orb_L	-3	57	-6	261	-5.3779
	CAU_L	0	3	3	85	-4.9138
	PCUN_R	12	-66	30	92	-4.0166

Note: pSS, primary Sjögren's syndrome; HC, healthy control; sfALFF, static fractional amplitude of low-frequency fluctuation; sReHo, static regional homogeneity; SMA_R, right supplementary motor area; Frontal_Med_Orb_L, left orbital middle frontal gyrus; CAU_L, left caudate nucleus; PCUN_R, right precuneus lobe; MNI; Montreal Neurological Institute

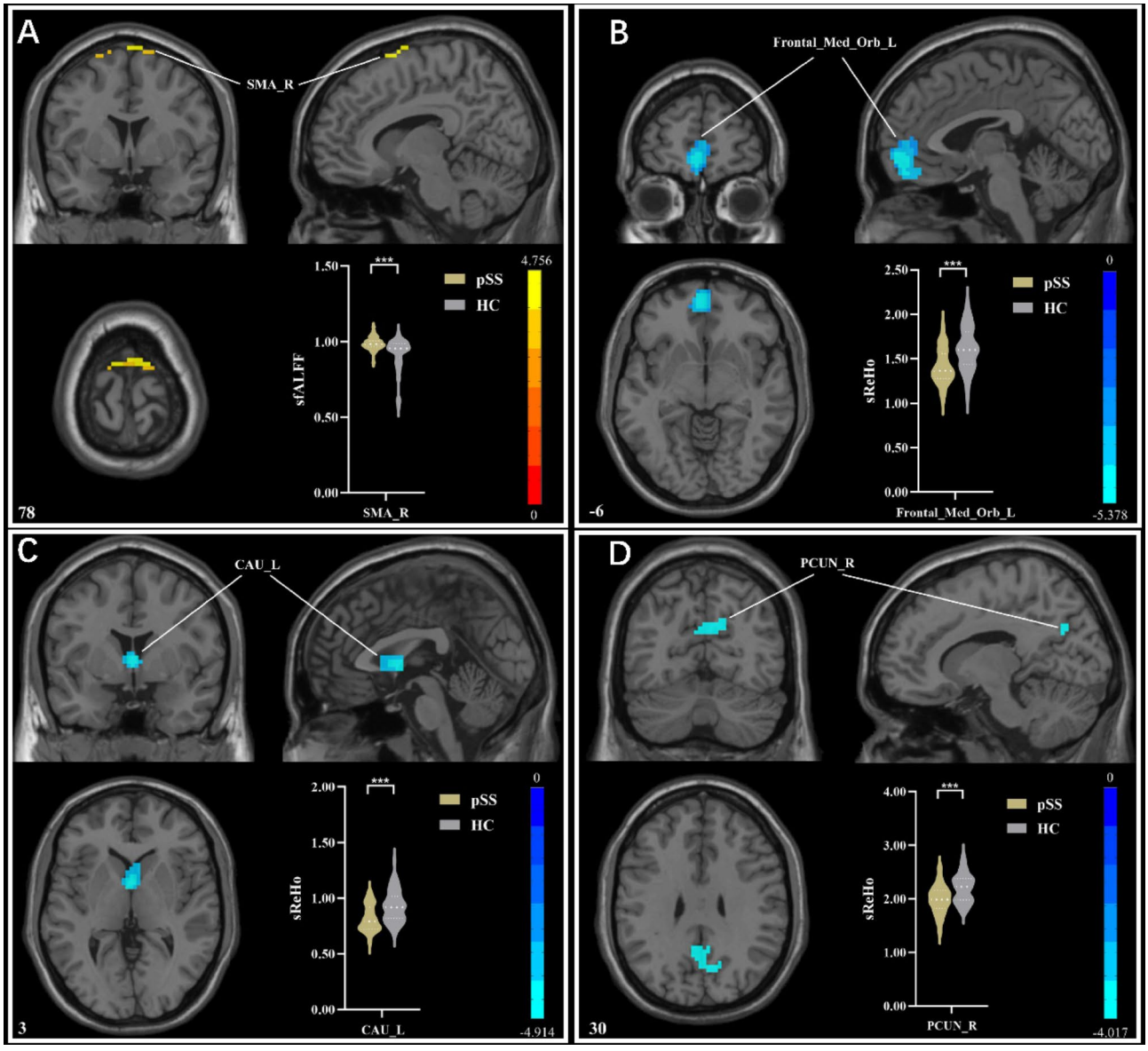

Fig. 2 Brain regions with significant alterations of sfALFF and sReHo between pSS and HC. Note: pSS, primary Sjögren's syndrome; HC, healthy control; sfALFF, static fractional amplitude of low-frequency fluctuation; sReHo, static regional homogeneity; SMA_R, right supplementary motor area; Frontal_Med_Orb_L, left orbital middle frontal gyrus; CAU_L, left caudate nucleus; PCUN_R, right precuneus lobe; *** indicates a significant level of $P < 0.001$, Bonferroni correction

Table 3 Brain regions with changed DfALFF and dReHo between the pSS and HC groups

Indices	Brain region	MNI coordinate			Voxels	Peak intensity
		X	Y	Z		
dfALFF	SMA_L	6	3	78	53	5.9228
dReHo	Frontal_Sup_R	24	57	0	92	4.3796

Note: pSS, primary Sjögren's syndrome; HC, healthy control; dfALFF, dynamic fractional amplitude of low-frequency fluctuation; dReHo, dynamic regional homogeneity; SMA_L, left supplementary motor area; Frontal_Sup_R, right dorsolateral superior frontal gyrus; MNI; Montreal Neurological Institute

subregion of the SMA, plays a key role in cognition and non-motor tasks [29, 30]. Notably, the SMA has not been reported in prior rs-fMRI studies of pSS, offering a potential focus for future CNS research.

The frontal lobe, particularly the prefrontal cortex, is critical for voluntary movement, higher cognition, and emotional regulation [31, 32]. The orbitofrontal cortex, linked to the limbic system, mediates emotional and cognitive processes, while the middle frontal gyrus supports

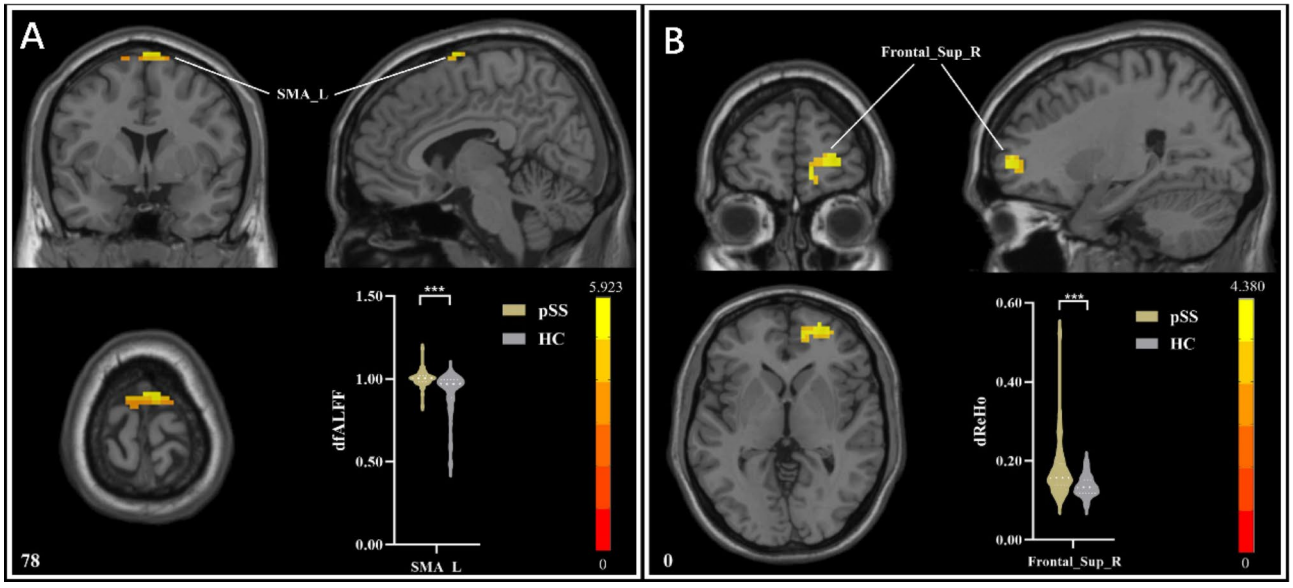

Fig. 3 Brain regions with significant alterations of dfALFF and dReHo between pSS and HC. Note: pSS, primary Sjögren's syndrome; HC, healthy control; dfALFF, dynamic fractional amplitude of low-frequency fluctuation; dReHo, dynamic regional homogeneity; SMA_L, left supplementary motor area; Frontal_Sup_R, right dorsolateral superior frontal gyrus; *** indicates a significant level of $P < 0.001$, Bonferroni correction

executive attention, decision-making, and motor planning [33, 34]. Previous studies have identified abnormal activity or connectivity in the frontal and frontoparietal regions of pSS patients [2, 7, 22, 35]. This study further supports the frontal lobe as a key abnormal region in pSS, with decreased sReHo in the left orbital middle frontal gyrus (Frontal_Med_Orb_L) suggesting reduced coherence and potential links to cognitive impairments such as attention, memory, and executive function deficits.

The caudate nucleus is a key component of the basal ganglia, collaborating with the cerebral cortex and cerebellum to regulate muscle tension and postural reflexes during voluntary movements. Previous studies by Kchaou et al. [36] reported a case of pSS with initial symptoms of bradykinesia and increased muscle tension, indirectly suggesting that pSS may have a certain impact on the function of the caudate nucleus. Additionally, the caudate nucleus is also connected with emotion control and learning memory. Tzarouchi et al. [2] found that the volume of the caudate nucleus in pSS patients decreased compared to HCs. Zhang et al. [7] found that the connectivity between the caudate nucleus and the cingulate gyrus increased in pSS patients, which may indicate brain network reorganization and neuroplasticity in pSS patients. This study utilized sReHo analysis of rs-fMRI and found reduced internal activity consistency in CAU_L of pSS patients, aligning with prior findings [2, 7]. We speculate it may be related to processing and executive control disorders, sensory processing deficits, and decreased emotional and learning regulation abilities in pSS patients.

The precuneus is a small square gyrus on the posterior medial surface of the parietal lobe of the brain, connected to various cortical and subcortical regions such as the frontal lobe, parietal lobe, and occipital lobe. It is involved in various functions, including visual spatial and visual motion integration, self-related information processing, and self-awareness [37]. Some parts of the precuneus also serve as core hubs of the default mode network [38], promoting processes such as resting state, attention regulation, and integration of higher cognition [39]. Currently, there are no studies reporting abnormal changes in the function of the precuneus in pSS patients. The finding of decreased sReHo values in PCUN_R of pSS patients in this study may be related to two factors: (1) visual-spatial and executive function decline due to dry eyes and optic neuritis [40, 41] and (2) emotional and cognitive impairments, including attention, memory, and emotional regulation deficits. Future multicenter studies with larger samples are needed to validate these findings.

Abnormal brain regions in DfALFF and dReHo

This study represents the first application of dynamic indices (dfALFF and dReHo) from rs-fMRI to analyze regional brain functional changes in pSS. The findings revealed increased dfALFF in SMA_L and increased dReHo in Frontal_Sup_R among pSS patients. Importantly, brain regions identified by dynamic indices differ from those identified by static indices, highlighting distinct sensitivities in detecting abnormalities across different brain regions. The combined use of both dynamic and static indices enhances the comprehensive study and mutual validation of pSS effects on the brain.

Table 4 Correlations between static and dynamic indicators with disease duration, treatment, laboratory indicators, and neuropsychological assessments

Indices	Brain region	MMSE	SAS	SDS	NCT-A	DST	IgG	IgA	IgM	C3	C4	SSB	SSA	Disease duration	Treatment
		r/P	*r/P*	*r/P*	*r/P*	*r/P*	*r/P*	*r/P*	*r/P*	*r/P*	*r/P*	*r/P*	*r/P*	*r/P*	*r/P*
sfALFF	SMA_R	-0.019/0.890	-0.087/0.577	0.209/0.178	-0.187/0.188	0.058/0.697	0.200/0.113	0.122/0.339	0.074/0.561	-0.050/0.697	-0.164/0.195	0.236/0.060	0.047/0.714	0.008/0.950	0.054/0.671
sReHo	Frontal_Med_Orb_L	0.062/0.655	-0.163/0.297	-0.113/0.471	-0.125/0.380	0.085/0.571	0.071/0.576	0.064/0.614	0.084/0.510	-0.134/0.289	-0.148/0.243	-0.112/0.378	0.033/0.794	-0.066/0.605	0.036/0.778
	Caudate_L	0.132/0.340	0.295/0.055	-0.037/0.815	-0.147/0.304	-0.082/0.584	-0.001/0.995	-0.012/0.924	0.134/0.292	-0.191/0.131	-0.060/0.638	0.115/0.365	0.102/0.420	-0.015/0.909	0.029/0.820
	Precuneus_R	-0.032/0.821	-0.133/0.395	-0.223/0.150	-0.389/**0.005***	0.266/0.071	0.122/0.337	-0.111/0.381	0.112/0.377	-0.134/0.290	-0.252/0.045	0.096/0.449	0.171/0.178	-0.130/0.307	-0.036/0.777
dfALFF	SMA_L	-0.109/0.434	-0.037/0.816	0.080/0.608	-0.096/0.501	0.168/0.253	0.187/0.139	0.131/0.301	0.137/0.279	-0.090/0.481	-0.128/0.312	0.286/0.022	0.062/0.625	-0.049/0.700	-0.081/0.527
dReHo	Frontal_Sup_R	-0.140/0.314	0.109/0.488	0.120/0.443	0.257/0.068	-0.390/**0.007***	-0.218/0.083	0.001/0.994	0.058/0.651	0.125/0.325	0.231/0.067	-0.108/0.394	-0.224/0.075	0.040/0.752	-0.004/0.976

Note: MMSE, Mini-Mental State Examination; SAS, Self-Rating Anxiety Scale; SDS, Self-rating Depression Scale; NCT-A, Number Connection Test-Type A; DST, Digit Symbol Test; sfALFF, static fractional amplitude of low-frequency fluctuation; sReHo, static regional homogeneity; dfALFF, dynamic fractional amplitude of low-frequency fluctuation; dReHo, dynamic regional homogeneity; SMA_R, right supplementary motor area; Frontal_Med_Orb_L, left orbital middle frontal gyrus; CAU_L, left caudate nucleus; PCUN_R, right precuneus lobe; SMA_L, left supplementary motor area; Frontal_Sup_R, right dorsolateral superior frontal gyrus; * indicates a significant level of $P < 0.008$

The SMA, identified by both dfALFF and sfALFF, may play a key role in pSS-related cognitive impairment. Importantly, these regions are situated on opposite sides—left and right—underscoring their mutual validation and complementarity. Previous studies have found that the left pre-SMA is believed to have a stronger response to happy and sad stimuli compared to neutral stimuli, suggesting a higher sensitivity of the left pre-SMA to emotional responses [42]. Therefore, the observed compensatory increase in left SMA activity in pSS patients might stem from diminished emotional regulation abilities, potentially leading to heightened emotional responses. However, this hypothesis remains speculative and requires further validation through additional studies.

The prefrontal cortex, particularly the right dorsolateral region, is critical for executive control, attention, and memory [32, 43, 44]. Increased dReHo in the right dorsolateral prefrontal cortex of pSS patients suggests its involvement in cognitive impairments, consistent with its role in higher cognitive functions and emotional regulation.

Correlations between certain brain regions and disease duration, treatment, laboratory indicators, and neuropsychological assessments

This study found a negative correlation between sReHo in PCUN_R and NCT-A scores in pSS patients. Reduced neuronal activity in PCUN_R correlates with longer digital connection times, consistent with cognitive impairment in pSS. This supports the precuneus as a key region in pSS-related cognitive dysfunction. Additionally, a negative correlation was observed between dReHo in Frontal_Sup_R and DST scores, indicating that lower task performance corresponds to higher neuronal activity in this region. We propose that this increased activity may reflect compensatory mechanisms [45–47].

The relationship between disease duration, laboratory indicators, and neurological involvement in pSS remains unclear. Some clinical studies suggest that disease duration, anti-Ro/SS-A and anti-La/SS-B antibody positivity, and low complement levels may be risk factors for neurological involvement in pSS patients [9, 48, 49]. However, neuroimaging studies have yielded conflicting results. Tzarouchi et al. [4] found no correlation between DTI-derived metrics and disease duration, Zhang et al. [50] reported no link between hippocampal functional connectivity and disease duration, and Lauvsnes et al. [51] observed no association between white matter volume and anti-SSA/SSB antibodies. This study aligns with these findings, as no significant correlations were found between disease duration, laboratory indicators, and abnormal brain regions. We hypothesize that these discrepancies may stem from differences in sample sizes

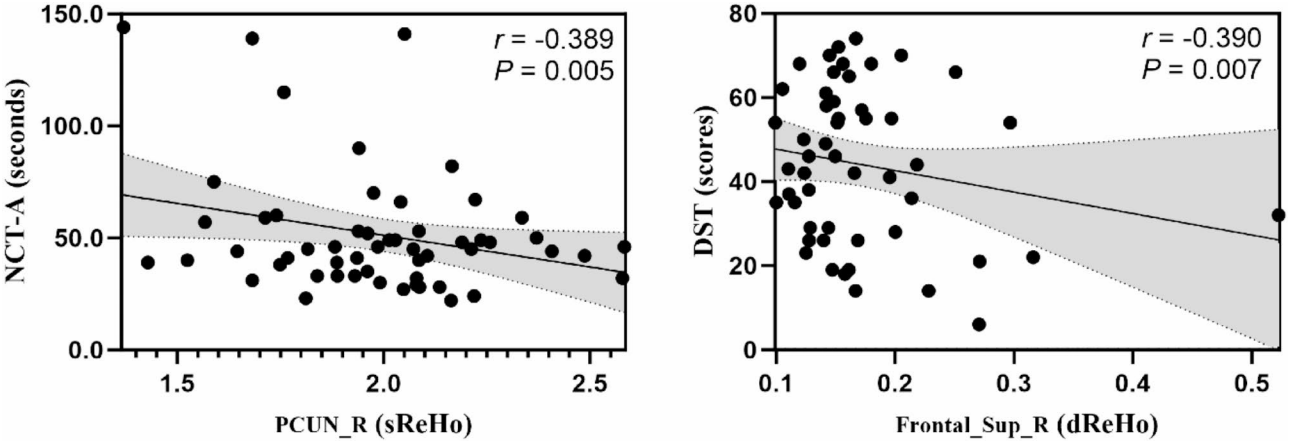

Fig. 4 Correlation between NCT-A and DST tests and brain regions which the sReHo and dReHo were changed in PSS patients

between clinical and imaging studies. Due to challenges in case recruitment, imaging studies often have significantly smaller sample sizes-sometimes one-tenth or less of those in clinical studies. Although this study includes the largest pSS imaging cohort to date, further expansion of the sample size is needed to improve the reproducibility and generalizability of the results. Additionally, the results of this study showed no significant correlation between treatment status and abnormal brain regions. This may also be related to the fact that current clinical treatments are not precisely targeted at the nervous system.

This study has several limitations. First, while pSS patients often experience fatigue and sleep disturbances in addition to cognitive impairment, these symptoms were not assessed due to patient compliance and time constraints. Scales such as the Pittsburgh Sleep Quality Index and the Fatigue Severity Scale were not included. Second, variations in disease activity or treatment regimens may influence brain functional changes in pSS. However, the limited sample size precluded exploration of these factors. Future studies should expand the sample size and stratify patients by disease stage to better understand neuropathological mechanisms. Third, this study was conducted at a single center, which may limit generalizability. Multicenter and interdisciplinary collaborations are needed to improve the accuracy and reproducibility of the findings.

Conclusion

In summary, pSS patients exhibit functional abnormalities in multiple brain regions, including an increase in sfALFF value of SMA_R, dfALFF value of SMA_L, and dReHo value of Frontal_Sup_R, while sReHo values of Frontal_Med_Orb_L, CAU_L, and PCUN_R decrease. It can be seen that static and dynamic indicators have different sensitivities in detecting abnormal activities in different brain regions. The combined application of both indicators is more conducive to the comprehensive study of local brain functional changes in pSS patients, offering imaging-based evidence for exploring potential central nervous system damage in this population.

Abbreviations

3D-T1WI	Three-dimensional T1-weighted imaging
ALFF	Amplitude of Low Frequency Fluctuations
BOLD	Blood oxygen level-dependent
CAU_L	Left caudate nucleus
CNS	Central nervous system
dfALFF	Dynamic fALFF
DPABI	Data Processing and Analysis of Brain Imaging
dReHo	Dynamic reHo
DST	Digit Symbol Test
DWI	Diffusion-weighted imaging
ESSDAI	EULAR Sjögren's Syndrome Disease Activity Index
fALFF	Low-frequency fluctuation
FOV	Field of view
Frontal_Med_Orb_L	Left orbital middle frontal gyrus
Frontal_Sup_R	Right dorsolateral superior frontal gyrus
FWHM	Full width at half maximum
HCs	Healthy controls
MMSE	Mini-Mental State Examination
NCT-A	Number Connection Test-Type A
PCUN_R	Right precuneus lobe
pSS	Primary Sjögren's syndrome
ReHo	Region homogeneity
rs-fMRI	Resting-state Functional Magnetic Resonance Imaging
SAS	Self-rating Anxiety Scale
SDS	Self-rating Depression Scale
sfALFF	Static fALFF
SMA_L	Left supplementary motor area
SMA_R	Right supplementary motor area
sReHo	Static ReHo
T1WI	T1-weighted imaging
T2	FLAIR, T2 fluid attenuated inversion recovery
T2WI	T2-weighted imaging
TE	Echo time
TR	Repetition time

Supplementary Information

The online version contains supplementary material available at https://doi.org/10.1186/s13075-025-03554-3.

Supplementary Material 1

Acknowledgements
Not applicable.

Author contributions
All authors were involved in the preparation of the article and approval of the version for submission. CH, LW, ZH and PW contributed equally and substantially to the conception, design, and drafting of the article of the study. CH and LW was responsible for language editing. JH, YS, XZ, XD and HC substantial contributions to the acquisition of data. ZH and PW revised the article critically for important intellectual content and final approval of the version of the article to be published.

Funding
This study was supported by the Zhejiang Provincial Medical and Health Technology Project (2021RC024).

Data availability
No datasets were generated or analysed during the current study.

Declarations

Ethics approval and consent to participate
The study was approved by the Research Ethics Committee (2021-023-01 and ZN-20230331-0053-01) and written informed consent was obtained for all subjects prior to inclusion.

Consent for publication
Not applicable.

Competing interests
The authors declare no competing interests.

Received: 24 July 2024 / Accepted: 6 April 2025
Published online: 23 April 2025

References

1. Chatzis L, Vlachoyiannopoulos PG, Tzioufas AG, Goules AV. New frontiers in precision medicine for Sjogren's syndrome. Expert Rev Clin Immunol. 2021;17(2):127–41.
2. Tzarouchi LC, Tsifetaki N, Konitsiotis S, Zikou A, Astrakas L, Drosos A, et al. CNS involvement in primary Sjogren syndrome: assessment of gray and white matter changes with MRI and voxel-based morphometry. AJR Am J Roentgenol. 2011;197(5):1207–12.
3. Andrianopoulou A, Zikou AK, Astrakas LG, Gerolymatou N, Xydis V, Voulgari P et al. Functional connectivity and microstructural changes of the brain in primary Sjögren syndrome: the relationship with depression. Acta radiologica (Stockholm, Sweden: 1987). 2020;61(12):1684-94.
4. Tzarouchi LC, Zikou AK, Tsifetaki N, Astrakas LG, Konitsiotis S, Voulgari P, et al. White matter water diffusion changes in primary Sjögren syndrome. AJNR Am J Neuroradiol. 2014;35(4):680–5.
5. Goulabchand R, Castille E, Navucet S, Etchecopar-Etchart D, Matos A, Maria A, et al. The interplay between cognition, depression, anxiety, and sleep in primary Sjogren's syndrome patients. Sci Rep. 2022;12(1):13176.
6. Segal BM, Mueller BA, Zhu X, Prosser R, Pogatchnik B, Holker E, et al. Disruption of brain white matter microstructure in primary Sjögren's syndrome: evidence from diffusion tensor imaging. Rheumatology (Oxford). 2010;49(8):1530–9.
7. Zhang XD, Li JL, Zhou JM, Lu ZN, Zhao LR, Shen W, et al. Altered white matter structural connectivity in primary Sjögren's syndrome: a link-based analysis. Neuroradiology. 2022;64(10):2011–9.
8. Zhang XD, Ke J, Li JL, Su YY, Zhou JM, Zhao LR et al. Different cerebral functional segregation in Sjogren's syndrome with or without systemic lupus erythematosus revealed by amplitude of low-frequency fluctuation. Acta radiologica (Stockholm, Sweden: 1987). 2022;63(9):1214-22.
9. Fan W, Par-Young J, Li K, Zhang Y, Xiao P, Hua L, et al. Clinical features and high-risk indicators of central nervous system involvement in primary Sjögren's syndrome. Clin Rheumatol. 2023;42(2):443–51.
10. Finn ES, Poldrack RA, Shine JM. Functional neuroimaging as a catalyst for integrated neuroscience. Nature. 2023;623(7986):263–73.
11. Wang L, Feng Q, Ge X, Chen F, Yu B, Chen B, et al. Textural features reflecting local activity of the hippocampus improve the diagnosis of Alzheimer's disease and amnestic mild cognitive impairment: a radiomics study based on functional magnetic resonance imaging. Front NeuroSci. 2022;16:970245.
12. Wang L, Feng Q, Wang M, Zhu T, Yu E, Niu J, et al. An effective brain imaging biomarker for AD and aMCI: ALFF in slow-5 frequency band. Curr Alzheimer Res. 2021;18(1):45–55.
13. Wu H, Sun C, Huang X, Wei R, Li Z, Ke D, et al. Short-range structural connections are more severely damaged in early-stage MS. AJNR Am J Neuroradiol. 2022;43(3):361–7.
14. Yan W, Palaniyappan L, Liddle PF, Rangaprakash D, Wei W, Deshpande G. Characterization of hemodynamic alterations in schizophrenia and bipolar disorder and their effect on resting-state fMRI functional connectivity. Schizophr Bull. 2022;48(3):695–711.
15. Ibrahim B, Suppiah S, Ibrahim N, Mohamad M, Hassan HA, Nasser NS, et al. Diagnostic power of resting-state fMRI for detection of network connectivity in Alzheimer's disease and mild cognitive impairment: a systematic review. Hum Brain Mapp. 2021;42(9):2941–68.
16. Zang YF, He Y, Zhu CZ, Cao QJ, Sui MQ, Liang M, et al. Altered baseline brain activity in children with ADHD revealed by resting-state functional MRI. Brain Dev. 2007;29(2):83–91.
17. Zang Y, Jiang T, Lu Y, He Y, Tian L. Regional homogeneity approach to fMRI data analysis. NeuroImage. 2004;22(1):394–400.
18. Yue J, Zhao N, Qiao Y, Feng ZJ, Hu YS, Ge Q, et al. Higher reliability and validity of wavelet-ALFF of resting-state fMRI: from multicenter database and application to rTMS modulation. Hum Brain Mapp. 2023;44(3):1105–17.
19. Wang M, Tang X, Li B, Wan T, Zhu X, Zhu Y, et al. Dynamic local metrics changes in patients with toothache: a resting-state functional magnetic resonance imaging study. Front Neurol. 2022;13:1077432.
20. Lv H, Wang Z, Tong E, Williams LM, Zaharchuk G, Zeineh M, et al. Resting-state functional MRI: everything that nonexperts have always wanted to know. AJNR Am J Neuroradiol. 2018;39(8):1390–9.
21. Liu P, Li Q, Zhang A, Liu Z, Sun N, Yang C, et al. Similar and different regional homogeneity changes between bipolar disorder and unipolar depression: a resting-state fMRI study. Neuropsychiatr Dis Treat. 2020;16:1087–93.
22. Xing W, Shi W, Leng Y, Sun X, Guan T, Liao W, et al. Resting-state fMRI in primary Sjögren syndrome. Acta Radiol (Stockholm Sweden: 1987). 2018;59(9):1091–6.
23. Ge X, Wang L, Pan L, Ye H, Zhu X, Fan S, et al. Amplitude of low-frequency fluctuation after a single-trigger pain in patients with classical trigeminal neuralgia. J Headache Pain. 2022;23(1):117.
24. Niu X, Gao X, Zhang M, Dang J, Sun J, Lang Y, et al. Static and dynamic changes of intrinsic brain local connectivity in internet gaming disorder. BMC Psychiatry. 2023;23(1):578.
25. Penfield W, Welch K. The supplementary motor area of the cerebral cortex; a clinical and experimental study. AMA Archives Neurol Psychiatry. 1951;66(3):289–317.
26. Nachev P, Kennard C, Husain M. Functional role of the supplementary and pre-supplementary motor areas. Nat Rev Neurosci. 2008;9(11):856–69.
27. Harika-Germaneau G, Rachid F, Chatard A, Lafay-Chebassier C, Solinas M, Thirioux B, et al. Continuous theta burst stimulation over the supplementary motor area in refractory obsessive-compulsive disorder treatment: a randomized sham-controlled trial. Brain Stimul. 2019;12(6):1565–71.
28. Hertrich I, Dietrich S, Ackermann H. The role of the supplementary motor area for speech and language processing. Neurosci Biobehav Rev. 2016;68:602–10.
29. Sjöberg RL, Stålnacke M, Andersson M, Eriksson J. The supplementary motor area syndrome and cognitive control. Neuropsychologia. 2019;129:141–5.
30. Schwartze M, Rothermich K, Kotz SA. Functional dissociation of pre-SMA and SMA-proper in temporal processing. NeuroImage. 2012;60(1):290–8.
31. Bush G. Cingulate, frontal, and parietal cortical dysfunction in attention-deficit/hyperactivity disorder. Biol Psychiatry. 2011;69(12):1160–7.
32. Bush G, Luu P, Posner MI. Cognitive and emotional influences in anterior cingulate cortex. Trends Cogn Sci. 2000;4(6):215–22.
33. Vernet M, Quentin R, Chanes L, Mitsumasu A, Valero-Cabré A. Frontal eye field, where art thou? Anatomy, function, and non-invasive manipulation of frontal regions involved in eye movements and associated cognitive operations. Front Integr Nuerosci. 2014;8:66.
34. Hu MY, Zhang LJ, Kang M, Pan YC, Ge QM, Li QY, et al. Brain activity in different brain areas of patients with dry eye during the female climacteric period according to voxel-based morphometry. Front Neurol. 2022;13:879444.
35. Le Guern V, Belin C, Henegar C, Moroni C, Maillet D, Lacau C, et al. Cognitive function and 99mTc-ECD brain SPECT are significantly correlated in patients

with primary Sjogren syndrome: a case-control study. Ann Rheum Dis. 2010;69(1):132–7.
36. Kchaou M, Ben Ali N, Hmida I, Fray S, Jamoussi H, Jalleli M et al. Parkinsonism and Sjögren's syndrome: a fortuitous association or a shared immunopathogenesis? Case reports in medicine. 2015;2015:432910.
37. Zhang S, Li CS. Functional connectivity mapping of the human precuneus by resting state fMRI. NeuroImage. 2012;59(4):3548–62.
38. Fuentealba-Villarroel FJ, Renner J, Hilbig A, Bruton OJ, Rasia-Filho AA. Spindle-shaped neurons in the human posteromedial (Precuneus) cortex. Front Synaptic Neurosci. 2021;13:769228.
39. Messina A, Cuccì G, Crescimanno C, Signorelli MS. Clinical anatomy of the precuneus and pathogenesis of the schizophrenia. Anat Sci Int. 2023;98(4):473–81.
40. Zhang Y, Lin T, Jiang A, Zhao N, Gong L. Vision-related quality of life and psychological status in Chinese women with Sjogren's syndrome dry eye: a case-control study. BMC Womens Health. 2016;16(1):75.
41. Qiao L, Wang Q, Fei Y, Zhang W, Xu Y, Zhang Y, et al. The clinical characteristics of primary Sjogren's syndrome with neuromyelitis optica spectrum disorder in China: a STROBE-compliant article. Medicine. 2015;94(28):e1145.
42. Rovetti J, Copelli F, Russo FA. Audio and visual speech emotion activate the left pre-supplementary motor area. Cogn Affect Behav Neurosci. 2022;22(2):291–303.
43. Krmpotich TD, Tregellas JR, Thompson LL, Banich MT, Klenk AM, Tanabe JL. Resting-state activity in the left executive control network is associated with behavioral approach and is increased in substance dependence. Drug Alcohol Depend. 2013;129(1–2):1–7.
44. Yang G, Wu H, Li Q, Liu X, Fu Z, Jiang J. Dorsolateral prefrontal activity supports a cognitive space organization of cognitive control. eLife. 2024;12.
45. Hu H, Wang L, Abdul S, Tang X, Feng Q, Mu Y, et al. Frequency-dependent alterations in functional connectivity in patients with Alzheimer's disease spectrum disorders. Front Aging Neurosci. 2024;16:1375836.
46. Fan Y, Wang L, Jiang H, Fu Y, Ma Z, Wu X, et al. Depression circuit adaptation in post-stroke depression. J Affect Disord. 2023;336:52–63.
47. Fishman I, Linke AC, Hau J, Carper RA, Müller RA. Atypical functional connectivity of amygdala related to reduced symptom severity in children with autism. J Am Acad Child Adolesc Psychiatry. 2018;57(10):764–e774763.
48. Massara A, Bonazza S, Castellino G, Caniatti L, Trotta F, Borrelli M, et al. Central nervous system involvement in Sjögren's syndrome: unusual, but not unremarkable–clinical, serological characteristics and outcomes in a large cohort of Italian patients. Rheumatology (Oxford). 2010;49(8):1540–9.
49. Konak HE, Gök K, Armağan B, Güven SC, Atalar E, Apaydın H, et al. Neurological involvement in patients with primary Sjögren's syndrome: a retrospective cross-sectional study. Ann Indian Acad Neurol. 2023;26(4):424–30.
50. Zhang XD, Zhao LR, Zhou JM, Su YY, Ke J, Cheng Y. Altered hippocampal functional connectivity in primary Sjögren syndrome: a resting-state fMRI study. Lupus. 2020;29(5):446–54.
51. Lauvsnes MB, Beyer MK, Appenzeller S, Greve OJ, Harboe E, Gøransson LG, et al. Loss of cerebral white matter in primary Sjögren's syndrome: a controlled volumetric magnetic resonance imaging study. Eur J Neurol. 2014;21(10):1324–9.

Publisher's note